

# Development of a New Nanotribometer with Multi Asperity Contact

Jérôme Dejeu <sup>Y,¶</sup>,  
Joël Abadie, Emmanuel Piat, Patrick Rougeot, Stéphane Oster <sup>Y</sup>  
Philippe Stempflé, Jamal Takadoum <sup>¶</sup>

femto-st Institute, UMR CNRS 6174 – ENSMM / UFC / UTBM,  
<sup>Y</sup> Automatic Control and Micro-Mechatronic Systems Department  
<sup>¶</sup> Micro Nano Sciences & Systems Department  
26 Chemin de l'épitaphe, 25030 Besançon Cedex

[emmanuel.piat@ens2m.fr](mailto:emmanuel.piat@ens2m.fr)

**Abstract:** It is often difficult to make a connection between the tribological properties really assessed for a single asperity and the ones which involve the whole asperities in a microcontact. We propose a new apparatus development based on passive diamagnetic levitation (PDL) that can be used to study friction in microcontact with a lower range of force than with classical nanotribometers. This sensor measures micro and nanoforces. Its sensitive part is a ten centimeters long glass capillary tube used as a horizontal levitating seismic mass (20 to 80 mg). This rigid part is connected to a magnetic spring with stiffness between 0.01 and 0.03 N/m. The measurement range is 100 $\mu$ N with a resolution between one and five nanonewton. In order to validate this sensor in a multi asperity nanotribological context, this part is used to measure tangential friction forces generated by spherical micro-objects sliding on flat substrate. Results are compared with the ones provided by a classical multiasperity nanotribometer.

**Key words:** nanotribometer, nano force sensor, diamagnetic levitation

## 1. INTRODUCTION

Manufactured products are getting smaller and smaller and are integrating more and more functionalities in small volumes. As a result of the size reduction, the influence of the surfaces increases dramatically, and hence the friction problem becomes more important, notably during some micro assembly processes [1]. Accurate micro and nano force measurement is necessary in order to study the friction at this scale. Such measurement problematic still remains an important challenge (especially if uncertainty

measurement must be guaranteed) and several international metrology laboratories work on new micro and nano force sensors development like the National Institut of Standards and Technology (NIST-USA) [2]. The nanotribology complexity is due to the fact that the resolution of problems related to friction and wear in micro systems cannot be realized by a simple transposition of the laws and experimental validations established at the macroscopic scale.

Thus, tribological properties in micromechanical systems are usually evaluated using a scanning probe microscope [3] or surface force apparatus [4] involving a mono-asperity or a circular

contact. However, it is often difficult to make a connection between the tribological properties really assessed for a single asperity and the ones which involve the whole asperities in a macrocontact. For instance, the friction coefficient obtained with an AFM in a mono-asperity context has little to do with the coefficient obtained in real microsystems because the last one implies a vast number of microcontacts which must be taken into account. Consequently, nanotribometers have been developed for this purpose in order to determine the friction force under very low contact pressures. However, there is still a gap between the load scales and the force range measurement achieved with an AFM (generally nN- $\mu$ N) and the ones of the current nanotribometers ( $\mu$ N - several mN).

In order to explore this gap, a new apparatus was developed in the femto-st Institute and used by researchers in tribology and microrobotics. This micro and nanoforce sensor is based on passive diamagnetic levitation (PDL) [5]. Like nanotribometers, it can be used to characterize multi asperity friction. The tangential forces that can be measured are between 0 and 100  $\mu$ N. The resolution is between 1 and 5 nanonewton. Thus the measured forces can be smaller than the ones usually measured by nanotribometers in a multi asperity context. The resolution and stiffness of this new force sensor is in the same range than an AFM with a thin cantilever but the force range is much larger. In order to validate this sensor for nanotribological characterization, a comparison of friction characterizations obtained with this sensor and the *CSM Nanotribometer* [6] (Peseux Switzerland) is presented.

## 2. EXPERIMENTAL DETAILS

### 2.1. Samples

- The minimal tangential force that is measurable with the CSM nanotribometer is 10 $\mu$ N with 1 $\mu$ N resolution. The CSM nanotribometer was used to characterize the friction between a

glass sphere and a glass substrate. Sample is a 1mm diameter glass sphere ;

- As the force sensor based on PDL can only push a microstructure on a substrate during the tangential force measurement, a specific structure made of three microspheres (instead of one sphere) was used in order to avoid rolling movement. Samples are glass microsphere with 100  $\mu$ m ( $\pm$  5 $\mu$ m) and 40  $\mu$ m ( $\pm$  2.8  $\mu$ m) diameters;

All spheres are provided by SPI Supplies and commercialized by Neyco (Paris, France). Diameters are certified using certified standards from the National Institute of Standards and Technology.

The flat glass substrates used are sold by Fischer Scientific. Before starting the friction experiment, the glass surface was cleaned in ethanol.

### 2.2. Glass spheres joining

For the friction experiment with the passive diamagnetic levitation nanotribometer, the glass spheres have been glued in order to realize different structures and to apply different load forces (due to weight structure).

The glass spheres structure has been assembled thanks to an experimental micromanipulation station (PRONOMIA platform [7]) and with the Dymax 628-VLV glue and the Blue Wave 50 apparatus (Dymax, Garches, France). Indeed, the glue was reticulated by UV light (365 nm). The different steps of the glass spheres joining are presented in the figure 9 and a video is available on the Institute website<sup>1</sup>.

First, two glass spheres were driven by the Silicon Finger Tips (Sifit) of the platform one against the other in order to form the first part of the desired structure (step 1). Second, a sphere was grasped (figure 1a), dipped into the glue (figure 1b) and positioned on top of the structure prepared in step 1 (figure 1c). Then, the sphere with the glue was put down on the structure (figure 1d), and the

---

<sup>1</sup> <http://www.femto-st.fr/fr/Departements-de-recherche/AS2M/Equipes-de-recherche/SAMMI/Themes/Stations-de-micro-assemblage/Collage-de-billes.php>

whole sphere assembly lighted by the UV light in order to stick the spheres together.

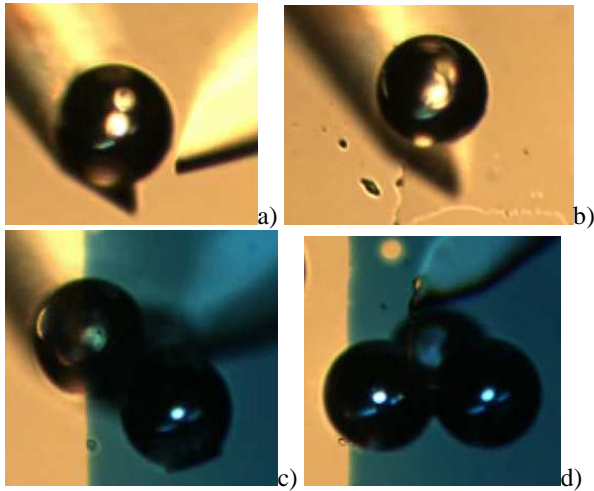


**Figure 1. Different steps of the glass sphere joining: a) glass gassed, b) dipped into the glue, c) glass positioning before joining, d) joining and final structure.**

An example of the different structures realized was presented figure 2. The load force applied on the silica surface is ranged between 800 nN and 40  $\mu$ N.

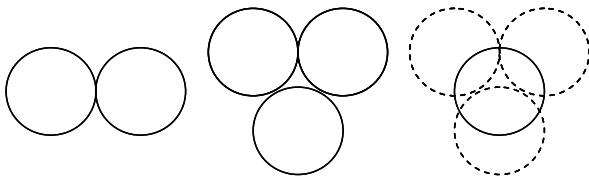


**Figure 2. Structured realized for the friction experiments on the passive diamagnetic levitation nanotribology.**

### 2.3. Passive nano force sensor prototype based on diamagnetic levitation

The new experimental device is based on a nanoforce sensor using a diamagnetic levitation principle. Contrary to classical nanoforce sensors based on monolithic elastic microstructures (AFM based force sensors, piezoresistive microforce sensors, capacitive microforce sensors, piezoelectric microforce sensors, etc.), the part of this sensor that is sensitive to the external force to be measured is a macroscopic seismic mass.

On force sensors based on elastic microstructures (generally microcantilevers), appropriate devices are used to measure a signal related to the deformation of the microstructure when an external force is applied to its end. Because maximum microstructure deformations are usually small, these sensors are mostly limited in range of force measurement but have large frequency bandwidth.

On force sensors using a rigid seismic mass, the force is applied to a mass whose displacements will be measured with appropriate devices. Because such displacements can be important with specific designs, a large range of force measurement is possible. Nano or microforce sensors based on this principle are nevertheless really uncommon, especially if the seismic mass is macroscopic. A force sensor with a range measurement of several millinewtons and based on a mass moving inside a pneumatic linear bearing is described in [8]. The mass is 21.17 grams and the force resolution is 0.5  $\mu$ N. The air friction inside the bearing is assumed small enough to be neglected.

#### 2.3.1 Levitating seismic mass

The apparatus presented here is a new design based on a rigid macroscopic seismic mass. This mass is a levitating capillary tube that is called *maglevtube* (see figure 3).

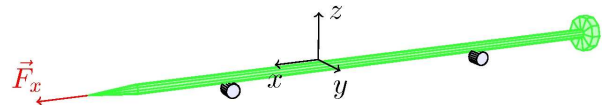


**Figure 3. Macroscopic seismic mass sensitive to external forces.**

This glass tube has a microscopic tip at one end like a micropipet on which the external force to be measured is applied. A plane deflector is stuck on the other end to facilitate the measurement of the  $x$  displacement of the tube. Two small magnets  $M_2$  are stuck on the tube. These magnets  $M_2$  levitate *passively* thanks to repulsive diamagnetic effects coupled with attractive magnetic effects.

The suspension mechanism  $L$  of a magnet  $M_2$  is given on figure 4. Two identical (material, geometry,...) magnets  $M_1$  and  $M_1'$  are used with north and south poles in opposite direction on the vertical axis.

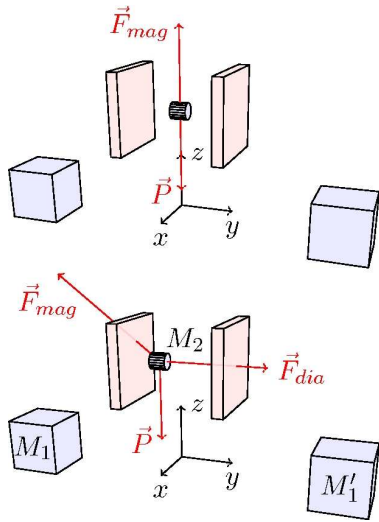


Figure 4. Passive suspension mechanism  $L$ .

The levitating magnet  $M_2$  is placed between the two fixed magnets such that the attractive forces  $\vec{F}_{mag}$  compensate the weight of  $M_2$ . The resulting equilibrium state is stable in the plan  $(\vec{x}, \vec{z})$  but unstable along  $\vec{y}$  because any slight displacement of  $M_2$  along  $\vec{y}$  will increase the  $\vec{y}$  component of the magnetic forces  $\vec{F}_{mag}$  and  $M_2$  will move towards  $M_1$  or  $M_1'$ . This unstable equilibrium is stabilized with the addition of two diamagnetic plates. It can be shown that  $\vec{F}_{dia}$  components along  $\vec{x}$  and  $\vec{z}$  are negligible, thus the diamagnetic forces  $\vec{F}_{dia}$  can be considered to be only along  $\vec{y}$  axis. Due to the intrinsic properties of diamagnetic materials,  $\vec{F}_{dia}$  is always opposed to the magnetic attraction along  $\vec{y}$  and will compensate any displacement along  $\vec{y}$ .

Figure 5 shows the levitating force sensing device. It uses two suspension mechanisms  $L_1$  and  $L_2$  spaced out in order to reduce the influence between each other. The two levitating magnets  $M_2$  are parts of the maglevtube. Thus this last one can be considered as a rigid seismic mass with a naturally stable equilibrium state with six degrees of freedom (dof). The maglevtube displacements along  $\vec{x}$  are measured with a confocal chromatic

sensor (STIL SA CL2, CL3 or CL4 optical pens associated to a CHR150-L controller) which is aimed at the deflector. This sensor is not shown on figure 5. The maglevtube mass is 74 mg on the real prototype.

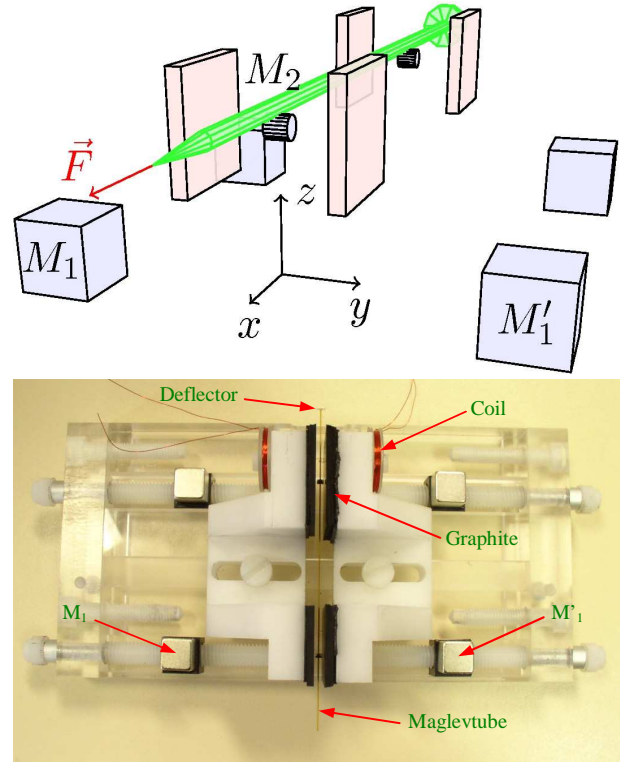
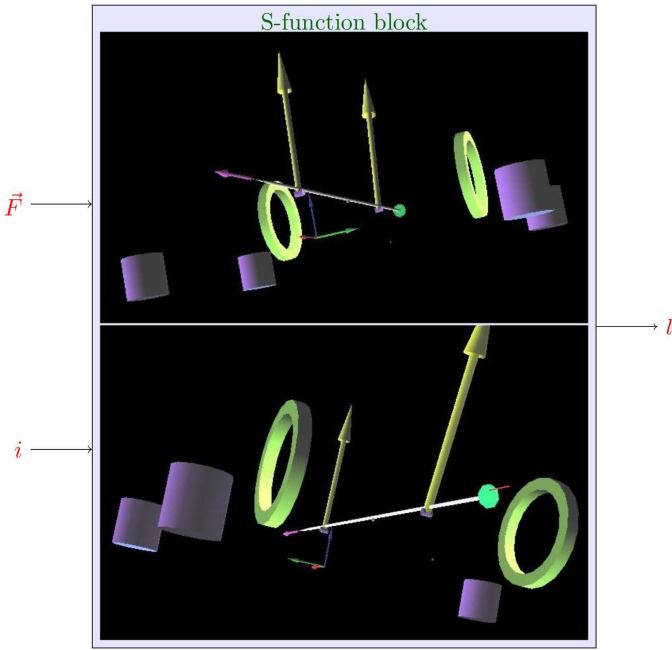


Figure 5. Force sensor schematic and real prototype.

### 2.3.2. Force sensing principle

When the maglevtube is moved away from its equilibrium position in the plan  $(\vec{x}, \vec{z})$ , the maglevtube returns to it because of the magnetic attractive force which depends on the maglevtube displacement. Therefore, the maglevtube is mechanically connected to a virtual *magnetic spring* with a given stiffness for each dof.

All the six dof of the maglevtube can be excited and exhibit particular trajectories. Because the levitation is similar to the behaviour of spacecrafts, the representation of the attitude of the maglevtube has been inspired by [7] (using quaternions for its modelling) and the non linear solving is implemented in a simulator under Matlab-Simulink (see figure 6).



**Figure 6. Simulink s-function block including 3D modelling and OpenGL rendering.**

This sensor is currently designed to only measure the force  $\vec{F}$  applied along the longitudinal  $\vec{x}$  axis of the tube (see figure 5). In this case, measured force is  $\vec{F} = F \vec{x}$ . As it is shown on figure 7, if the rigid maglevtube is excited in the simulator along  $\vec{x}$  with a force  $F$  equal to  $1 \mu\text{N}$ , it will converge to its steady state with a badly damped dynamic because the viscous friction due to the air is small. Along  $\vec{x}$ , the obtained dynamic is very closed to a linear second order dynamic (see section 2.3.3).

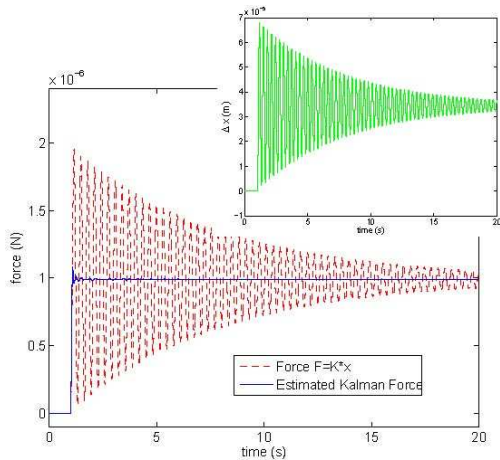


**Figure 7. Simulated dynamic along x for a step force  $F_x = 1 \mu\text{N}$  and associated force estimation using deconvolution.**

If the magnetic spring stiffness along  $\vec{x}$  axis is called  $K_x$  the component  $F$  to be measured will generate in steady state a displacement  $\Delta x$  of the *maglevtube* with the following relation:

$$F = K_x \Delta x. \quad (1)$$

The measurement of the displacement  $\Delta x$  is called  $l$  and is done with the confocal chromatic sensor. In the  $x$  direction, the sensor has an excellent linearity and the stiffness  $K_x$  can be assumed to be constant for  $\pm 1 \text{ mm}$  longitudinal displacements of the maglevtube (see figure 8). Equation (1) can't be used if steady state is not reached. To estimate the force in this case, it is necessary to deconvolve the measured displacement  $\Delta x$  to take into account the badly damped dynamic of the maglevtube. This deconvolution stage is done using a Kalman filter.

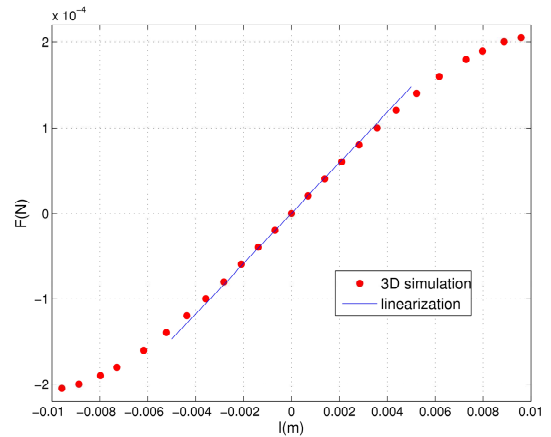


**Figure 8. Simulated static force (F) / displacement (l) characteristic along  $\vec{x}$  axis.**

### 2.3.3 Sensor calibration

Calibration is a complex problem for micro and nano force sensors because of the lack of standard forces at this scale [6]: no international measurement institute supports a direct force realization linked to the International System of Units (SI) below  $1 \text{ N}$ , even for static force. Thus, calibration must be performed using indirect static or dynamic approaches and care must be taken with stiffness calculation. Several dynamic

calibration methods have been investigated for force sensors using seismic mass. These methods are based on particular external force generation like impact force [10-11], step force [12] and oscillating force [13-15]. The chosen calibration approach is based on a zero input force response (ZIR) and only requires a pulse current in coils located at the suspension mechanism  $L_2$  (see figure 3) to briefly change the magnetic field and to set the maglevtube into free damped oscillations along  $\bar{x}$  axis with unknown initial conditions. Then, in the following maglevtube dynamic state model:

$$\begin{bmatrix} \dot{x} \\ \ddot{x} \end{bmatrix} = \begin{bmatrix} 0 & 1 \\ -\frac{K_x}{m} & -\frac{K_v}{m} \end{bmatrix} \begin{bmatrix} x \\ \dot{x} \end{bmatrix} + \begin{bmatrix} 0 \\ \frac{1}{m} \end{bmatrix} F$$

$$y = \begin{bmatrix} 1 & 0 \end{bmatrix} \begin{bmatrix} x \\ \dot{x} \end{bmatrix} + v$$

unknown parameters  $K_x$  (stiffness) and  $K_v$  (viscous friction coefficient) are identified from the measured output signals  $y$  (disturbed by a gaussian additive noise  $v$ ) given by the confocal chromatic sensor. This identification process is performed using Matlab Identification Toolbox (state variable identification from ZIR with unknown initial conditions). Figure 9 shows the matching between the measured zero input response along  $\bar{x}$  axis and the reconstructed linear one with the model identified. Typical stiffness obtained is  $0.01 \text{ N.m}^{-1}$ . This stiffness can be adjusted by changing the distance between magnets  $M_1$  and  $M_1'$  in  $L_1$  and  $L_2$ .

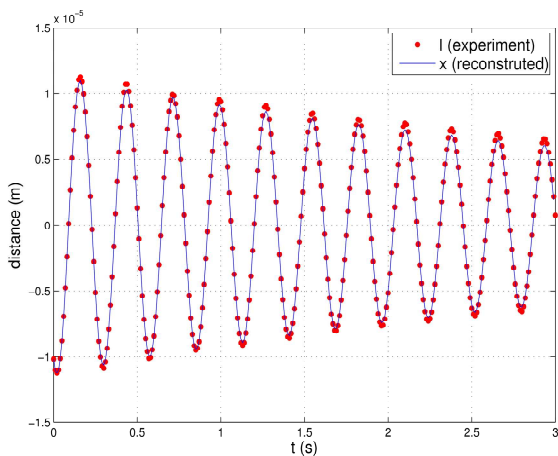


Figure 9. Measured and identified zero input response of the maglevtube.

#### 2.4. Experimental setup for static friction characterisation

After the identification step, the force  $F$  is calculated using the distance  $\Delta l$  measured by the confocal sensor. This sensor is connected to a Dspace signal processor via a RS232 link. The datas are sent to the Dspace at 100Hz. A simulink model is running on the Dspace and calculates the force  $F$  (deconvolution stage). A picture of the experiments are presented figure 10.

Static friction characterization consists in moving the glass substrate along  $\bar{x}$  axis until the glass spheres structure comes into contact with the tip of the maglevtube. Then the tangential friction force generated by the displacement of the glass substrate is measured in real time by the Dspace system. The motion of glass substrate is provided by three PI motorized translation stages. This whole setup in running under a Guppy camera to provide position feedbacks of the glass spheres structures and the maglevtube.

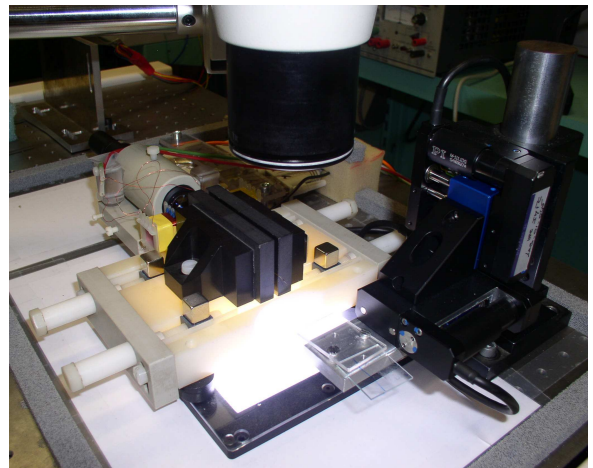
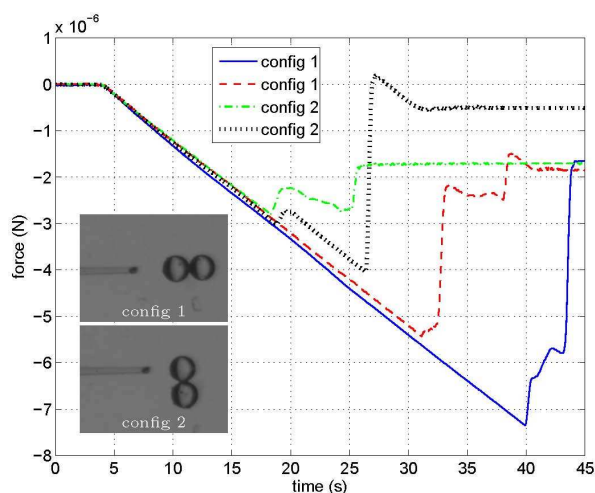


Figure 10. Experimental setup.

### 3. RESULTS & DISCUSSION

Different examples of friction force measured by the PDL nanotribometer are presented figure 11 and 12 for different structures.



**Figure 11. Friction force measured by the PDL nanotribometer between a glass substrate and two stuck glass sphere of 100  $\mu\text{m}$ .**

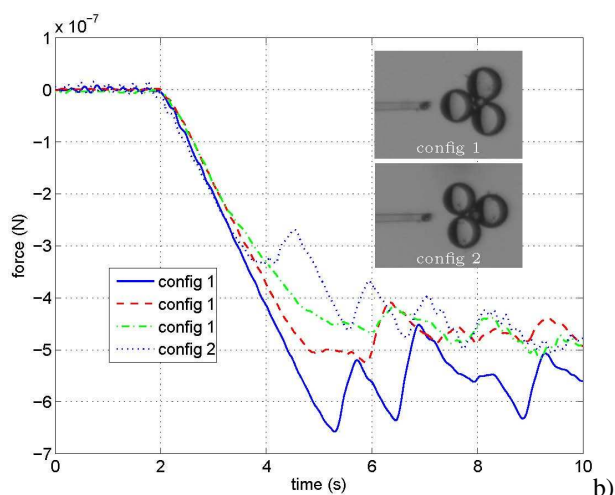
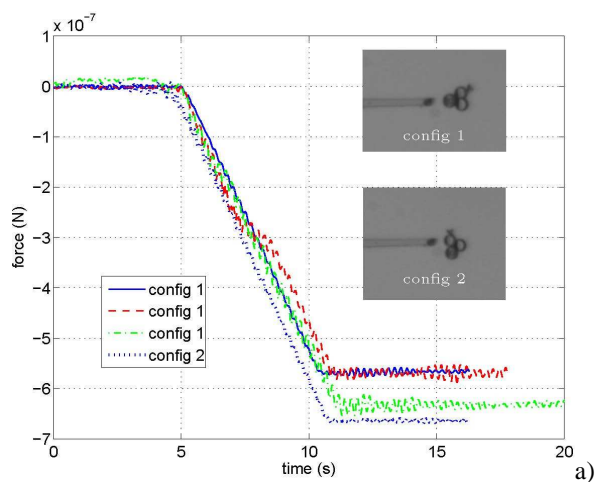


**Figure 12. Friction force measured by the PDL nanotribometer between glass substrate and three stuck glass spheres with different sizes: a) 40  $\mu\text{m}$ , b) 100  $\mu\text{m}$ .**

After the first peak which corresponds to the static friction coefficient, the force measured depends on the glass sphere structure used. Indeed, in figure 11, the peaks series observed are due to sphere displacements by rolling or jumping (observed by the Guppy camera, but not shown in this paper and available on the Institute website<sup>2</sup>). After the peak, in figure 12, the force stays near the same value that involves sphere sliding on the glass substrate (Video available on Institute website<sup>2</sup>) and makes possible the determination of the dynamic friction coefficient.

Figures 11 and 12 shows that the tangential force measured depends on the contact point between the maglevtube end and the glass spheres structure used. This is explained, for structures with two spheres, by the fact that the pushing location on one sphere involves a rotation of this sphere around the other sphere, and thus the tangential force is not the same.

The tangential force obtained with the PDL force sensor, is compared with the one obtained using the CSM nanotribometer [16]. Experiments with the latter are performed with a normal load equal to 10 mN (corresponding to a maximal Hertzien pressure about 250 MPa) in order to obtain a “similar” Hertzien pressure during the two experiments. CSM nanotribometer results are presented figure 13 for two speeds (one sphere friction).

The tangential force measured by the CSM nanotribometer is higher than with the PDL force sensor – i.e respectively 3mN instead of a few  $\mu\text{N}$  – because the difference between the normal loads. So, the friction coefficient is assessed in order to compare the results.

The static and dynamic coefficient frictions determined with the two nanotribometers are summarized on table 1. To estimate these values with the PDL force sensor, the tangential force is

<sup>2</sup> <http://www.femto-st.fr/fr/Departements-de-recherche/AS2M/Equipes-de-recherche/SAMMI/Projets/Nanotribologie.php>

measured by the levitation apparatus and the normal force is the glass spheres weight (estimated with their diameters).

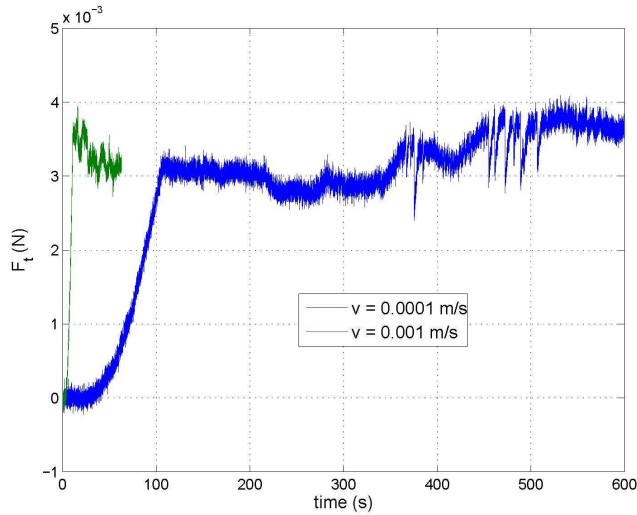


**Figure 13. Friction force measured by the CSM nanotribometer using a glass substrate and a 1 mm glass sphere.**

**Table 1. Friction coefficient obtained for different glass sphere size and structures.**

CSM Nanotribometer (*) PDL nanotribometer (**)			
Number of glass sphere	Size of glass sphere	Hertz Pressure (MPa)	Friction coefficient
1	1 mm	250	0.307*
	40 $\mu\text{m}$	93	0.220**
	100 $\mu\text{m}$	126	0.156**
2	40 $\mu\text{m}$	93	0.097-
	100 $\mu\text{m}$	126	0.272**
3	40 $\mu\text{m}$	93	0.243**
	100 $\mu\text{m}$	126	0.016**

The reference value is the one determined by using the CSM nanotribometer. So, for the PDL nanotribometer, the weaker value obtained when pushing one sphere can be explained by the rolling movement which decrease the static force. The capillarity force predominance – due to the hydrophilic surfaces – can probably explain the

difference on the friction coefficient between spheres with 40 and 100  $\mu\text{m}$  diameter.

Furthermore, the values for two and three spheres, obtained with the PDL force sensor, are close to the one obtained with the CSM nanotribometer, excepted for three 100  $\mu\text{m}$  diameter sphere. The variation of the friction coefficient for two spheres is correlated with the pushing location. Indeed, in the configuration 2, shown on figure 11, the structure rolls and rotates and so the friction is weak.

An important influence of the sphere diameter is observed on the friction coefficient for the three spheres structures. Several assumptions can be made to account this difference. First the glass substrate cleaning procedure is not optimized. Indeed, a piranha solution must be used in place of ethanol. Second, the substrate was hydrophilic, so the normal force must be corrected in order to take into account the capillarity effect as demonstrated by Hild *et al.* [17]. Third, the contact point between the maglevtub and the glass sphere is not controlled (notably z positioning which is very critical). Fourth, some glue residue can stay on the glass spheres is the friction area.

#### 4. CONCLUSIONS

In this paper, we have presented a new nanotribometer based on a PLD force sensor. The first experiments have shown the influence of several parameters like the structure sliding on the substrate, the glass size, and the contact point between the maglevtub and the glass spheres. The apparatus development will continue with the introduction of a lateral camera in order to control the z contact point position. The structured realization with spheres in order to slide on the substrate must be improved. At the same time, a new apparatus that enable the control of the load force is under development.



## 5. ACKNOWLEDGEMENTS

This work is supported by the French National Research Agency (ANR) under STIL $\mu$ FORCE contract ANR-07-ROBO-0005: Study and development of micro and nanoforce stations for the industrial.

## 6. REFERENCES

- [1] S. Bargiel, K. Rabenorosoa, C. Clévy, C. Gorecki et P. Lutz., **Towards micro-assembly of Hybrid MOEMS components on reconfigurable silicon freespace micro-optical bench**, Journal of Micromechanics and microengineering, vol 20(4), march 2010.
- [2] Gates, R.S., Pratt, J.R., **Prototype cantilevers for SI-traceable nanonewton force calibration**, Measurement Science And Technology, 2006, 7, 2852–2860
- [3] Szlufarska, I., Chandross, M., Carpick, R.W., **Recent advances in single-asperity nanotribology**, J. Phys. D:Appl. Phys., 2008, 41, 123001
- [4] Kumacheva, E., **Interfacial friction measurement in Surface force apparatus**, Progress in Surface Science, 1998, 58(2), 75-120
- [5] Boukallel, M., Piat, E., Abadie, J., **Passive diamagnetic levitation : theoretical foundations and application to the design of a micro-nano force sensor**, in Proc. of the IEEE/RSJ International Conference on Intelligent Robots and Systems, IROS'2003, 2003, 1062–1067.
- [6] Stempfle, P., Takadoum, J., **Micro Nanotribological studies of silicon and CNx coatings: Crystallography-induced anisotropy in friction and seizure**, The 14th Nordic Conference on Tribology, Luleå, 2010
- [7] Hériban, D., Gauthier, M., Gendreau, D., **Modular Robotic Platform for Silicon Micromechanical Components Assembly**, on proc. of the 6th int. Workshop on Microfactories, Evanston, Illinois, USA, October 2008
- [8] Fujii, Y., **Method for generating and measuring the micro-Newton level forces**, Mechanical Systems and Signal Processing, 2006, 20, 1362-1371
- [9] Wertz, J.R., editor, **Spacecraft Attitude Determination and Control**, D. Reidel, Dordrecht, Springer, Holland, 1978
- [10] Fujii, Y., Fujimoto, H., **Proposal for an impulse response evaluation method for force transducers**, Measurement Science and Technology, 1999, 10 (4), N31-N33
- [11] Fujimoto, H. and Fujii, Y., **Measurement of step impulse response of a force transducer**, Measurement Science and Technology, 2003, 14 (1), 65-69
- [12] Fujii, Y., **Proposal for a step response evaluation method for force transducers**, Measurement Science and Technology, 2003, 14 (10), 1741-1746
- [13] Fujii, Y., **A method for calibrating force transducers against oscillation force**, Measurement Science and Technology, 2003, 14 (8), 1253-1264
- [14] Kumme, R., **Investigation of the comparison method for the dynamic calibration of force transducers**, Measurement, 1998, 23, 239-245
- [15] Park, Y.K., Kumme, R., Kang, D.I., **Dynamic investigation of a three-component force-moment sensor**, Measurement Science and Technology, 2002, 13, 654-659
- [16] Scherge, M., **Scale dependance of friction**, World Tribology Congress WTC, Vienne, 2001, 31-37;
- [17] Hild, W. et al, **Microtribological properties on silicon and silicon coating with self-assembled monolayer : effect of applied load and sliding velocity**, tribology letters, 2007, 25(1), 1-7